

Entangling independent photons by time measurement

MATTHÄUS HALDER*, ALEXIOS BEVERATOS, NICOLAS GISIN, VALERIO SCARANI, CHRISTOPH SIMON AND HUGO ZBINDEN

Group of Applied Physics, University of Geneva, 20, rue de l'Ecole-de-Médecine, 1211 Geneva 4, Switzerland

*e-mail: matthaeus.halder@physics.unige.ch

Published online: 19 August 2007; doi:10.1038/nphys700

Entanglement is at the heart of quantum physics, both for its conceptual foundations and for applications in quantum communication. Remarkably, entanglement can be ‘swapped’: if we prepare two independent entangled pairs A1–A2 and B1–B2, a joint measurement on A1 and B1 (called a ‘Bell-state measurement’, BSM) has the effect of projecting A2 and B2 onto an entangled state, although these two particles have never interacted nor share any common past^{1,2}. Entanglement swapping with photon pairs has already been experimentally demonstrated^{3–6} using pulsed sources—where the challenge was to achieve sufficiently sharp synchronization of the photons in the BSM—but never with continuous-wave sources, as originally proposed². Here, we present an experiment where the coherence time of the photons exceeds the temporal resolution of the detectors. Hence, photon timing can be obtained by the detection times, and pulsed sources can be replaced by continuous-wave sources, which do not require any synchronization^{6,7}. This allows for the first time the use of completely autonomous sources, an important step towards real-world quantum networks with truly independent and distant nodes.

The BSM is the essential element in an entanglement-swapping experiment. Linear optics allows the realization of only a partial BSM⁸ by coupling the two incoming modes on a beam splitter and observing a suitable detection pattern in the outgoing modes. Such a measurement is successful in at most 50% of the cases. Still, a successful partial BSM entangles two photons that were, up to then, independent. The physics behind this realization is the bosonic character of photons. It is therefore crucial that the two incoming photons are indistinguishable: they must be identical in their spectral, spatial, polarization and temporal modes at the beam splitter; spectral overlap is achieved by the use of similar filters, spatial overlap by the use of single-mode optical fibres and polarization is matched by a polarization controller. In addition, the temporal resolution must be unambiguous: detection at a time $t \pm \Delta t_d$, where Δt_d is the temporal resolution of the detector, must single out a unique time mode. In previous experiments, synchronized pulsed sources created both of the photons at the same time and path lengths had to be matched to obtain the required temporal overlap. The pulse length, that is, the coherence length of the photons, was $\tau_c \ll \Delta t_d$ (typically $\tau_c < 1$ ps), but two subsequent pulses were separated by more than Δt_d (ref. 9). The drawback of such a realization is that the two sources cannot be totally autonomous, because of the indispensable synchronization. For the case where $\tau_c > \Delta t_d$ (ref. 10), the detectors always single out a unique time mode. As a benefit, we can give up the pulsed

character of the sources and the synchronization between them. By implementing this, we realize for the first time the entanglement swapping scheme as originally proposed in ref. 2.

The experimental scheme is shown in Fig. 1. Each of the two nonlinear crystals emits pairs of energy–time entangled photons¹¹ produced by spontaneous parametric down conversion (SPDC) of a photon originating from a continuous-wave laser. A pair can be created at any time t , and all of these processes are coherent within the km-long coherence length of the laser: $|\psi\rangle_A \propto \sum_t |t, t\rangle_A$ describes a pair of signal and idler photons emitted by source A at time t . Thus, the state produced by two independent sources can conveniently be represented as

$$|\Psi\rangle_{\text{prep}} = |\psi\rangle_A |\psi\rangle_B \propto \sum_t \left[|t, t\rangle_A |t, t\rangle_B + \sum_{\tau > 0} (|t, t\rangle_A |t + \tau, t + \tau\rangle_B + |t + \tau, t + \tau\rangle_A |t, t\rangle_B) \right].$$

The first term in the above sum describes four photons all arriving at the same time t at a beam splitter. Because for this case two identical photons bunch in the same mode, owing to their bosonic nature, this term leads to a Hong–Ou–Mandel (HOM) dip¹² (see below). The second term describes two photon pairs arriving with a time difference $\tau > 0$.

A partial BSM of photons A1 and B1 is realized by sending them through a 50/50 beam splitter and two detectors in the output modes⁸. When one of the detectors fires at time t and the other one at time $t + \tau$, this corresponds to a measurement of A1 and B1 in the Bell-state $|\Psi^-\rangle$ for time-bin qubits¹³. Consequently, the remaining two photons A2 and B2 are projected in the state $|\psi\rangle_{A_2 B_2} \equiv |\Psi^-\rangle_{A_2 B_2} \propto |t\rangle_{A_2} |t + \tau\rangle_{B_2} - |t + \tau\rangle_{A_2} |t\rangle_{B_2}$, which is a singlet state for time-bin entanglement. Hence, entanglement has been swapped. This process can be seen as teleportation^{14–18} of entanglement. Unlike former experiments, time bins here are not created by a pulse passing through an unbalanced interferometer with path length difference Δl (and $\tau = \Delta l/c$), but rather via post-selection. In our case, photons are created at arbitrary times, but only those that are detected with a temporal delay of τ are taken into account.

We now describe our experiment in more detail. Above, we have assumed that the detection times t and $t + \tau$ of the BSM are sharply defined. In physical terms, this requirement means that the detection times have to be determined with sub-coherence-time precision: this is the key ingredient that makes it possible to achieve

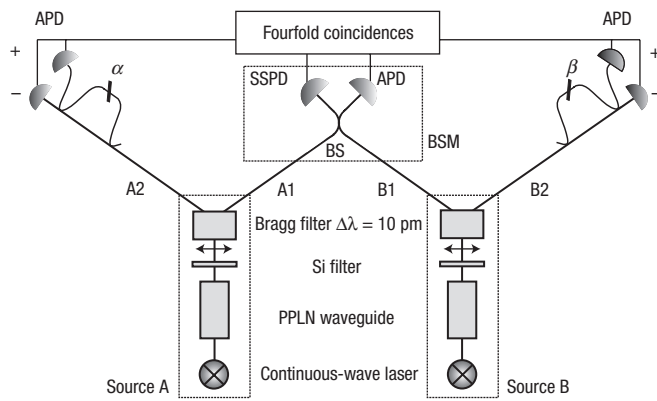


Figure 1 Schematic diagram of the experimental set-up. Two pairs of entangled photons (A1–A2 and B1–B2) are produced, one by each source (A and B), and all of the photons are narrowly filtered (10 pm). One photon of each pair (A1 and B1) is sent into a 50/50 beam splitter (BS) and both undergo a partial BSM. By detecting them in different output ports of the beam splitter with detectors SSPD and APD, and with a certain time delay τ , they are in the Ψ^- -state, which projects the two remaining photons (A2, B2) on the Ψ^- -state as well. The entanglement, swapped onto the photon pair A2–B2, is tested by passing them through interferometers with phases α and β , and detecting them by single-photon APDs in both outputs (+, –) of each interferometer.

synchronization of photons A1 and B1 by detection, and thus to use continuous-wave sources. As single-photon detectors have a certain intrinsic minimal jitter, the coherence length of the photons has to be increased to exceed this value by narrow filtering.

Consider the case where each of the two sources emits one entangled pair of photons, and where A1 and B1 take different exits from the beam splitter. The photon that takes output port 1 is detected by a niobium nitride (NbN) superconducting single-photon detector (SSPD)¹⁹ with a time resolution $\Delta t_d = 74$ ps. The photon in output port 2 is detected by an InGaAs single-photon avalanche diode (APD, $\Delta t_d = 105$ ps) triggered by the detection in the SSPD. The time resolution of these detectors is several times smaller than that of commercial telecommunication photon detection modules. To obtain a coherence length of the photons exceeding Δt_d , 10-pm-bandwidth filters are used, which corresponds to a coherence time τ_c of 350 ps. The induced losses are compensated for by the high down-conversion efficiency of periodically poled lithium niobate (PPLN) waveguide crystals²⁰ of 5×10^{-7} per pump photon and per nanometre of the created spectrum. For 2 mW of laser power, an emission flux, q , of 2×10^{-2} pairs per coherence time is obtained. Note that q is independent of the filtered bandwidth: in fact, narrower filtering decreases the number of photons per second but increases their coherence time by the same factor, hence keeping q constant.

Any two-detector click in the BSM prepares the two remaining photons in a time-bin entangled state. In our experiment, the creation rate for entangled photon pairs is $\approx 10^4$ s⁻¹, with time delays, τ , between photon A1 and B1 ranging from 0 to 10 ns. This is two orders of magnitude larger than in previous experiments at shorter and similar wavelengths^{3–6}. To verify entanglement between photons A2 and B2, they are sent through unbalanced Michelson interferometers (a and b) in a Franson configuration¹¹. The path length differences, Δl , of the interferometers must be identical only within the coherence length of the analysed photons (7 cm), but stable in phase (α and β), which is achieved by active stabilization²¹. Both output ports of each interferometer are connected to InGaAs

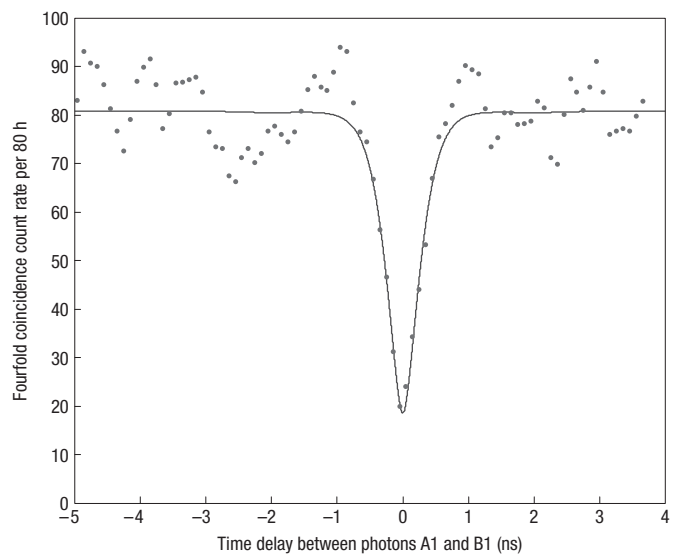


Figure 2 Fourfold coincidence count rate as a function of the temporal delay τ . For the photons A1 and B1 arriving simultaneously ($\tau = 0$) at the beam splitter, the coincidence rate decreases owing to photon bunching, which leads to a HOM dip of 77% visibility.

APDs, triggered by the detection of the photons in the BSM. As Δl of these analysing interferometers is fixed, only entanglement of pairs A2–B2 corresponding to $\tau = \Delta l/c$ can be tested. All of the other entangled pairs with $\tau' \neq \tau$ escape this analysis. Hence, our final count rate is two orders of magnitude smaller than the rate of created entangled pairs.

Fourfold coincidences, between one click in each BSM detector and one behind each interferometer, are registered by a multistop time-to-digital converter and the arrival times ($t, t + \tau$) are stored in a table. For $\tau = 0$, we observe a decrease in this coincidence count rate (see Fig. 2). The visibility, V , of this HOM dip indicates the degree of indistinguishability of the two photons A1 and B1. If, for higher time accuracy, two SSPDs are used in the BSM, a HOM dip of $V = 77\%$ is observed. (See the Methods section for a detailed discussion of the imperfect visibility.) The width of the dip corresponds to the convolution of τ_c for the two photons with the jitter of the detectors. Note that photons that are detected after the beam splitter at measurable different times, but within τ_c , do still partially bunch, which confirms that the relevant time precision is set by the coherence time of the photons. For the entanglement swapping experiment, we decided to use only one SSPD and an InGaAs APD in the BSM for its higher detection efficiency.

As usual for the analysis of time-bin entanglement¹³, interference is observable in the case where, at the output of the interferometers, both photons are detected at the same time. The interferometers erase the time information and temporally distinguishable events (at t and $t + \tau$ respectively) interfere^{10,13,22}. Changing the relative phase $\alpha - \beta$ between the interferometers leads to interference fringes in the coincidence count rates. We measured the four possible fourfold coincidence count rates $R_{ij}(\alpha, \beta)$ (clicks in two outer detectors conditioned on a successful BSM) with $i, j \in \{+, -\}$ being the different detectors behind interferometer a and b , respectively. Thus, the two-photon spin-correlation coefficient

$$E(\alpha, \beta) = \frac{R_{++}(\alpha, \beta) - R_{+-}(\alpha, \beta) - R_{-+}(\alpha, \beta) + R_{--}(\alpha, \beta)}{R_{++}(\alpha, \beta) + R_{+-}(\alpha, \beta) + R_{-+}(\alpha, \beta) + R_{--}(\alpha, \beta)}$$

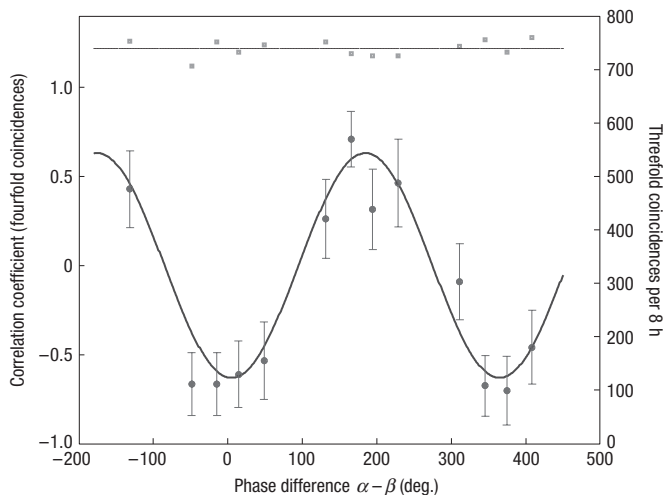


Figure 3 Correlation coefficient $E(\alpha, \beta)$ for detection of A2 and B2. E is plotted as a function of the relative phase $\alpha - \beta$ of the interferometers for coincidence events conditioned on a BSM of photon pair A1–B1 (circles). A fit (solid curve) of the form $E(\alpha, \beta) = V \cos(\alpha - \beta)$ gives a visibility $V = 0.63 \pm 0.02$, which proves successful entanglement swapping (see text). The coincidence count rate of only one detector conditioned on a successful BSM (threefold coincidence) is independent of the phase setting as expected for a Ψ^- state (squares). The error bars are determined by the Poisson distribution—that is, they are the square root of the obtained count rates.

is obtained as a function of the phase settings α and β and plotted in Fig. 3 for fixed α . A fit of the form $E(\alpha, \beta) = V \cos(\alpha - \beta)$ to our experimental data gives a visibility $V = 0.63 \pm 0.02$. If we assume that the two photons are in a Werner state (which corresponds to white noise), we can show that $V > 1/3$ is sufficient to demonstrate entanglement^{5,23}. Our experimental visibility clearly exceeds this bound. The squares show that the threefold coincidence count rate between a successful BSM and only one of the outside detectors is independent of the phase setting, as expected for a Ψ^- -state.

The integration time of this measurement was 1 h for each of the 13 phase settings and the experiment was run 8 times, and hence took 104 h, which demonstrates the stability of our set-up. Such long integration times are necessary because of low count rates (five fourfold coincidences per hour), which are mainly due to poor coupling efficiencies of the photons into optical fibres, losses in optical components such as filters and interferometers, as well as the limited detectors efficiencies. All of these factors decrease the probability of detecting all four photons of a two-pair event. Improving the coupling efficiency would allow shorter measurement times and lower q , and hence better visibility (see the discussion in the Methods section).

Time-bin entanglement is particularly stable and well suited for fibre-optic communications²⁴, and the coherence length of 7 cm allows tolerance of significant fibre length fluctuations as expected in field experiments. If count rates are also further improved, long-distance quantum communication²⁵ or quantum relays^{26,27} become realistic.

METHODS

EXPERIMENTAL DESCRIPTION OF THE SET-UP

Both sources consist of an external-cavity diode laser in continuous-wave mode at 780.027 nm (Toptica DL100), stabilized against a rubidium transition (D2-line of ⁸⁵Rb), pumping a nonlinear PPLN waveguide⁸ (HC Photonics) at a power of 2 mW. The process of SPDC creates 4×10^{11} pairs of photons per

second with a spectral width of 80 nm full-width at half-maximum centred at 1,560 nm. The photons are emitted collinearly and coupled into a single-mode fibre with 25% efficiency and the remaining laser light is blocked with a silicon high-pass filter (Si). Signal and idler photons are separated and filtered down to a bandwidth of 10 pm by custom-made tunable phase-shifted Bragg gratings (AOS GmbH). These filters have a rejection of > 40 dB, 3 dB insertion losses and can be tuned independently over a range of 400 pm. Once a signal photon has been filtered to ω_s , the corresponding idler photon has a well-defined frequency ω_i , owing to stabilized pump wavelength and energy conservation in the process of SPDC ($\omega_s + \omega_i = \omega_{\text{laser}}$). After filtering, the effective conversion efficiency for creating a photon pair within these 10 pm is 5×10^{-9} per pump photon. In principle, the available pump power permits us to produce narrow-band entangled photon pairs at rates of up to 3×10^8 pairs per second, which translates to an emission flux of more than 0.1 photons per coherence time. In this experiment, we limited the laser to 2 mW, to reduce the probability of multiple pair creation, which would decrease the interference visibility²⁸.

After the beam splitter, the first photon is detected by a NbN superconducting single-photon detector (Scontel) operated in free-running mode¹⁹, with a total detection efficiency of 4.5%, 300 dark counts per second and a timing resolution of 74 ps, including the time jitter of both the detector and the amplification and discrimination electronics. The second photon is detected by an InGaAs single-photon avalanche diode operated in Geiger mode and actively triggered by the detection in the SSPD. With home-made electronics this detector has a time jitter of 105 ps. The observed HOM dip with a visibility of 77% was obtained with two SSPD detectors, which were used because of their smaller time jitter. For the entanglement swapping, we used an APD, because of its higher efficiency, to shorten the integration time.

Photons A2 and B2 are also detected by InGaAs APDs (ID200, idQuantique). The APDs have quantum efficiencies of 30% and dark-count probabilities of 10^{-4} ns^{-1} . The interferometers are actively stabilized against a laser locked on an atomic transition, have a path length difference $\tau = \Delta l/c$ of 1.2 ns and insertion losses of 4 dB each. The relative phase $\alpha - \beta$ is varied, by keeping α fixed and scanning β .

DISCUSSION OF THE IMPERFECT VISIBILITY

Assuming a gaussian wave function $\psi(t, t') \propto e^{-2\ln 2(t-t')^2/\tau_c^2}$ for each photon pair (with $\tau_c = 350$ ps) and a gaussian detector jitter with $\Delta t_d = 70$ ps full-width at half-maximum for the SSPD, we find that the expected visibility reduction of the observed HOM dip due to the finite detector resolution is only of the order of 3%. This means that the detectors resolution is adequate for the present experiment. However, there are other imperfections. On the basis of a simple model with discrete time units of order τ_c , inspired by ref. 29, we estimate that multiple pair creation leads to a reduction in visibility of the order of $4q \approx 8\%$. Moreover, a frequency difference of the two photons due to fluctuations in the central wavelength of the filters (which we observed experimentally to be less than 5 pm) accounts for a reduction of visibility of the order of 3%. This means that for a difference corresponding to half the filters' bandwidth, only a slight loss in visibility is observed. We can explain this by the fact that detection of a photon with 70 ps time resolution projects its frequency uncertainty to the order of 50 pm, much larger than the displacement of 5 pm. Concerning the remaining error (of the order of 9% for the HOM dip), we believe that it is caused by polarization fluctuations due to long integration times and statistical fluctuations due to low count rates.

The further visibility reduction of the correlation coefficient in the entanglement swapping experiment can be explained by fluctuations and losses in the analysing interferometers during the long measurement time.

Received 2 April 2007; accepted 19 July 2007; published 19 August 2007.

References

1. Yurke, B. & Stoler, D. Bell's-inequality experiments using independent-particle sources. *Phys. Rev. A* **46**, 2229–2234 (1992).
2. Żukowski, M., Zeilinger, A., Horne, M. A. & Ekert, A. K. "Event-ready-detectors" Bell experiment via entanglement swapping. *Phys. Rev. Lett.* **71**, 4287–4290 (1993).
3. Pan, J.-W., Bouwmeester, D., Weinfurter, H. & Zeilinger, A. Experimental entanglement swapping: Entangling photons that never interacted. *Phys. Rev. Lett.* **80**, 3891–3894 (1998).
4. Jennewein, T., Weihs, G., Pan, J.-W. & Zeilinger, A. Experimental nonlocality proof of quantum teleportation and entanglement swapping. *Phys. Rev. Lett.* **88**, 017903 (2002).
5. de Riedmatten, H., Marcikic, I., Tittel, W., Zbinden, H. & Gisin, N. Long-distance entanglement swapping with photons from separated sources. *Phys. Rev. A* **71**, 050302 (2005).
6. Yang, T. et al. Experimental synchronization of independent entangled photon sources. *Phys. Rev. Lett.* **96**, 110501 (2006).
7. Kaltenbaeck, R., Blauensteiner, B., Żukowski, M., Aspelmeyer, M. & Zeilinger, A. Experimental interference of independent photons. *Phys. Rev. Lett.* **96**, 240502 (2006).

8. Weinfurter, H. Experimental Bell-state analysis. *Europhys. Lett.* **25**, 559–564 (1994).
9. Bouwmeester, D. *et al.* Experimental quantum teleportation. *Nature* **390**, 575–579 (1997).
10. Legero, T., Wilk, T., Henrich, M., Rempe, G. & Kuhn, A. Quantum beat of two single photons. *Phys. Rev. Lett.* **93**, 070503 (2004).
11. Franson, J. D. Bell inequality for position and time. *Phys. Rev. Lett.* **62**, 2205–2208 (1989).
12. Hong, C. K., Ou, Z. Y. & Mandel, L. Measurement of subpicosecond time intervals between two photons by interference. *Phys. Rev. Lett.* **59**, 2044–2046 (1987).
13. Brendel, J., Gisin, N., Tittel, W. & Zbinden, H. Pulsed energy–time entangled twin-photon source for quantum communication. *Phys. Rev. Lett.* **82**, 2594–2597 (1999).
14. Furusawa, A. Unconditional quantum teleportation. *Science* **282**, 706–709 (1998).
15. Boschi, D., Branca, S., De Martini, F., Hardy, L. & Popescu, S. Experimental realization of teleporting an unknown pure quantum state via dual classical and Einstein-Podolsky-Rosen channels. *Phys. Rev. Lett.* **80**, 1121–1125 (1998).
16. Marcikic, I., de Riedmatten, H., Tittel, W., Zbinden, H. & Gisin, N. Long-distance teleportation of qubits at telecommunication wavelengths. *Nature* **421**, 509–513 (2003).
17. Riebe, M. *et al.* Deterministic quantum teleportation with atoms. *Nature* **429**, 734–737 (2004).
18. Barrett, M. D. *et al.* Deterministic quantum teleportation of atomic qubits. *Nature* **422**, 412–415 (2003).
19. Milostnaya, I. *et al.* Superconducting single-photon detectors designed for operation at 1.55- μm telecommunication wavelength. *J. Phys. Conf. Ser.* **43**, 1334–1337 (2006).
20. Tanzilli, S. *et al.* PPLN waveguide for quantum communication. *Eur. Phys. J. D* **18**, 155–160 (2002).
21. Marcikic, I. *et al.* Distribution of time-bin entangled qubits over 50 km of optical fiber. *Phys. Rev. Lett.* **93**, 180502 (2004).
22. Pittman, T. B. *et al.* Can two-photon interference be considered the interference of two photons? *Phys. Rev. Lett.* **77**, 1917–1920 (1996).
23. Peres, A. Separability criterion for density matrices. *Phys. Rev. Lett.* **77**, 1413–1415 (1996).
24. Thew, R. T., Tanzilli, S., Tittel, W., Zbinden, H. & Gisin, N. Experimental investigation of the robustness of partially entangled qubits over 11 km. *Phys. Rev. A* **66**, 062304 (2002).
25. Duan, L.-M., Lukin, M. D., Cirac, J. I. & Zoller, P. Long-distance quantum communication with atomic ensembles and linear optics. *Nature* **414**, 413–418 (2001).
26. Jacobs, B. C., Pittman, T. B. & Franson, J. D. Quantum relays and noise suppression using linear optics. *Phys. Rev. A* **66**, 052307 (2002).
27. Collins, D., Gisin, N. & de Riedmatten, H. Quantum relay for long distance quantum cryptography. *J. Mod. Opt.* **522**, 735–753 (2005).
28. Scarani, V., de Riedmatten, H., Marcikic, I., Zbinden, H. & Gisin, N. Four-photon correction in two-photon Bell experiments. *Eur. Phys. J. D* **32**, 129–138 (2005).
29. de Riedmatten, H. *et al.* Two independent photon pairs versus four-photon entangled states in parametric down conversion. *J. Mod. Opt.* **51**, 1637–1649 (2004).

Acknowledgements

We thank C. Barreiro, J.-D. Gautier, G. Gol'tsman, C. Jorel, S. Tanzilli and J. van Houwelingen for technical support, and H. de Riedmatten, S. Iblisdir and R. Thew for helpful discussions. Financial support by the EU projects QAP and SINPHONIA and by the Swiss NCCR Quantum Photonics is acknowledged.

Correspondence and requests for materials should be addressed to M.H.

Competing financial interests

The authors declare no competing financial interests.

Reprints and permission information is available online at <http://npg.nature.com/reprintsandpermissions/>